

## STATISTICAL PROPERTIES OF RADIO EMISSION FROM THE PALOMAR SEYFERT GALAXIES

JAMES S. ULVESTAD

National Radio Astronomy Observatory

P.O. Box O, Socorro, NM 87801; julvesta@nrao.edu

AND

LUIS C. HO

The Observatories of the Carnegie Institution of Washington

813 Santa Barbara St., Pasadena, CA 91011; lho@ociw.edu

ApJ Vol. 558, in press

## ABSTRACT

We have carried out an analysis of the radio and optical properties of a statistical sample of 45 Seyfert galaxies from the Palomar spectroscopic survey of nearby galaxies. We find that the space density of bright galaxies ( $-22 \text{ mag} \leq M_{B_T} \leq -18 \text{ mag}$ ) showing Seyfert activity is  $(1.25 \pm 0.38) \times 10^{-3} \text{ Mpc}^{-3}$ , considerably higher than found in other Seyfert samples. Host galaxy types, radio spectra, and radio source sizes are uncorrelated with Seyfert type, as predicted by the unified schemes for active galaxies. Approximately half of the detected galaxies have flat or inverted radio spectra, more than expected based on previous samples. Surprisingly, Seyfert 1 galaxies are found to have somewhat stronger radio sources than Seyfert 2 galaxies at 6 and 20 cm, particularly among the galaxies with the weakest nuclear activity. We suggest that this difference can be accommodated in the unified schemes if a minimum level of Seyfert activity is required for a radio source to emerge from the vicinity of the active nucleus. Below this level, Seyfert radio sources might be suppressed by free-free absorption associated with the nuclear torus or a compact narrow-line region, thus accounting for both the weakness of the radio emission and the preponderance of flat spectra. Alternatively, the flat spectra and weak radio sources might indicate that the weak active nuclei are fed by advection-dominated accretion disks.

*Subject headings:* galaxies: active — galaxies: Seyfert — quasars: general — radio continuum: galaxies

## 1. INTRODUCTION

In the 1970s, significant numbers of Seyfert galaxies were first identified by means of the Markarian surveys of ultraviolet-excess objects, the last of which was published by Markarian, Lipovetskij, & Stepanian (1981). Since then, a variety of Seyfert samples have been developed, including heterogeneous samples derived from literature searches, and others selected based on specific observational criteria. Over the last 25 years, a number of researchers have performed arcsecond-resolution interferometric radio surveys of the galaxies in these samples. Among the most important radio surveys or compilations are those published by de Bruyn & Wilson (1976, 1978), Meurs & Wilson (1984), Ulvestad & Wilson (1984a, 1984b, 1989), Unger et al. (1987), Roy et al. (1994), Kukula et al. (1995), Nagar et al. (1999), Morganti et al. (1999), Thean et al. (2000, 2001), and Schmitt et al. (2001a,b). A comprehensive description of the observations, as well as possible selection effects in the different samples, is given by Ho & Ulvestad (2001).

The purposes of studying large statistical samples of Seyfert galaxies are many. Such studies can provide important tests of the ubiquity and applicability of “unified schemes” for Seyfert galaxies (Antonucci 1993; Wills 1999). In these schemes, the active nucleus is powered by a massive compact object, presumed to be a black hole, surrounded by an accretion disk or torus, and many observed properties of the galaxies are determined by the observer’s line of sight relative to the torus. The Seyfert 1 galaxies, with broad permitted optical emission lines, are those in which the torus is viewed closer to face-on orientation. The Seyfert 2 galaxies lack broad permitted lines, except (in at least some cases) in polarized flux (Antonucci & Miller

1985; Tran 1995; Moran et al. 2000), and are thought to be seen with the line of sight passing through the torus in an orientation closer to edge-on. In general, the centimeter-wavelength emission from Seyfert nuclei is thought to be unobscured, and so should have the same power when the torus is viewed from any angle. However, if that emission is predominantly due to radio jets, those jets should be viewed closer to end-on in Seyfert 1 galaxies. In this case, the nuclear radio sources might tend to have smaller apparent sizes than in Seyfert 2 galaxies, although this could be complicated by the fact that the end-on objects also could have higher surface brightness and be detected more easily.

Recently, Ho & Ulvestad (2001) used the Very Large Array (VLA) to image 52 nearby Seyfert galaxies selected from the Palomar spectroscopic survey of nearby galaxies (Ho, Filippenko, & Sargent 1995, 1997a, 1997b; Ho et al. 1997c), and presented the detailed observational data from that sample. The sample members were chosen from 486 bright northern galaxies typically having  $B_T \leq 12.5 \text{ mag}$ ; the sample is complete to  $B_T = 12.0 \text{ mag}$ , and 80% complete to  $B_T = 12.5 \text{ mag}$ . The spectroscopic observations (Ho et al. 1995) employed varying integration times, with each target observed long enough to reach an approximately uniform equivalent-width limit of 0.25 Å for H $\alpha$  emission (Ho et al. 1997a). Ho & Ulvestad (2001) have argued that this sample was uniformly selected and is expected to be unbiased relative to many other Seyfert galaxy samples studied in the literature. In this paper, we assess the statistical properties of the radio emission from this sample, including both the comparisons between Seyfert types and the overall correlations with a large set of galaxy properties.

## 2. THE RADIO DATA AND THE SAMPLE

The radio observations of the Palomar Seyfert sample were described in detail by Ho & Ulvestad (2001), but are briefly summarized here for completeness. Each of the galaxies in the sample was observed at two wavelengths, 6 and 20 cm, with the VLA (Thompson et al. 1980). The integration time on each galaxy at each wavelength ranged from 15 to 18 minutes, yielding a typical rms noise of  $40 \mu\text{Jy beam}^{-1}$ . Scaled arrays were used, to achieve a maximum resolution of approximately  $1.^{\prime\prime}1$  at the two wavelengths; this corresponds to a resolution of 110 pc at the typical galaxy distance of  $\sim 20$  Mpc. Full-resolution and tapered images were produced for each galaxy, with the tapered images having respective beam sizes of about  $2.^{\prime\prime}5$  and  $3.^{\prime\prime}6$ . Radio sizes and position angles of the nuclear sources were measured, and the flux densities also were found for both the unresolved cores and any resolved emission associated with the active nucleus. (Note that extended radio emission apparently associated with the host galaxy rather than with the active nucleus was not included.) The results of the radio measurements were tabulated by Ho & Ulvestad (2001), together with other properties of the host galaxies; those tabulated data form the primary numerical input to the studies reported in this paper.

The formal definition of the Palomar survey includes all bright ( $B_T \leq 12.5$  mag) northern ( $\delta > 0^\circ$ ) galaxies selected from the Revised Shapley-Ames Catalog of Bright Galaxies (RSA; Sandage & Tammann 1981). A total of 52 Seyfert galaxies were imaged with the VLA by Ho & Ulvestad (2001), most of which fit into the two primary selection criteria. However, three galaxies (NGC 1068, NGC 1358, and NGC 1667) had negative declinations, so they should be excluded from the statistical sample. In addition, a few other Seyferts fainter than the formal magnitude limit were imaged. These galaxies were included in the original sample either because of historical interest or because their apparent magnitudes had been revised slightly since the RSA was published (Ho et al. 1995). For our statistical sample, we have chosen to eliminate four galaxies with current measurements of  $B_T > 12.64$  mag: NGC 1167, NGC 3185, NGC 4169, and NGC 5548. At brighter magnitudes, the completeness corrections for the RSA are relatively minor and well established (Sandage, Tammann, & Yahil 1979). Therefore, the final statistical sample of Palomar Seyferts, studied in the rest of this paper, includes a total of 45 galaxies. Of these, 20 are type 1 Seyferts (defined to include all those types showing detectable broad-line emission, from type 1.0 through 1.9), and 25 are type 2 Seyferts.

## 3. STATISTICAL PROPERTIES AND CORRELATIONS WITH SEYFERT TYPE

A large number of properties of the Seyfert radio sources have been studied statistically. The statistical studies made use of an array of tests for censored data based on the package ASURV described by Isobe & Feigelson (1990) and by LaValley, Isobe, & Feigelson (1992). We generally use Gehan's Generalized Wilcoxon Test (hereafter "Gehan-Wilcoxon test") to assess possible differences between two samples. This test is used to define the probability that two samples drawn from the same parent population would have a difference as large as that observed in a particular parameter. The generalized Kendall's  $\tau$  coefficient is used to assess correlations between two variables. Distance-dependent quantities in this paper are based on a Hubble constant of  $H_0 = 75 \text{ km s}^{-1} \text{ Mpc}^{-1}$ ; when necessary, comparison samples from the literature have been converted to this

distance scale. In the subsections below, we present the results of various tests and some comparisons to previously published results for Seyfert samples.

### 3.1. Galaxy Distances

The median distance of the parent sample of Palomar galaxies is 18.2 Mpc (Ho et al. 1997a). Histograms of the distances of the galaxies classified as Seyferts are given in Figure 1; the median distances are 17.0 Mpc for the type 1 Seyferts and 20.4 Mpc for the type 2 Seyferts. These typical distances are considerably smaller than for most samples of Seyfert galaxies studied at radio wavelengths. For example, the distance-limited sample studied by Ulvestad & Wilson (1989) has a median distance of approximately 35 Mpc, while the CfA sample (Huchra & Burg 1992) has a median distance of 80 Mpc. The Gehan-Wilcoxon test shows that the distances of the two Seyfert types in the Palomar sample would differ by the observed amount 54% of the time if they were drawn from the same parent sample; thus, there are no significant distance biases between the two Seyfert types, which conceivably could cause systematic effects in quantities such as their radio luminosities.

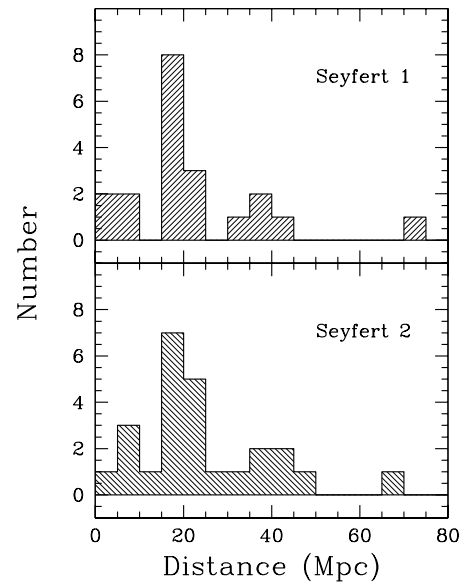


FIG. 1.— Histogram of galaxy distances in the Palomar Seyfert sample.

### 3.2. Host-Galaxy Types

Ho & Ulvestad (2001) gave host-galaxy morphological types for all the objects in the Palomar Seyfert sample. After removing the peculiar galaxy NGC 1275, whose morphology is ambiguous, the remaining 44 objects have been tested to see if there is any difference between the host-galaxy types of the type 1 and type 2 Seyferts. The Gehan-Wilcoxon test shows a 48% probability that the host galaxy types of the type 1 and type 2 Seyferts would differ as much as observed if they were drawn from the same parent sample, so there is no significant correlation between galaxy type and Seyfert class. As noted by Ho et al. (1997b), 4 of the 45 Palomar Seyferts reside in elliptical host galaxies. Often Seyfert galaxies are defined to be in spiral hosts, but this is not a requirement of the definition of Seyfert galaxies used for the Palomar sample, in spite of the classical "lore" that all Seyferts are in spiral galaxies.

### 3.3. Optical Luminosities

The apparent and absolute magnitudes of the Palomar Seyferts have been tabulated by Ho & Ulvestad (2001), and can be used to derive an optical luminosity function. To do so, we have used the  $V/V_{\max}$  method (Schmidt 1968; Huchra & Sargent 1973; Condon 1989), correcting for the incompleteness of the RSA catalog as specified by Sandage et al. (1979); the maximum completeness correction is a factor of 1.5. Errors have been estimated using the method described by Condon (1989). Table 1 gives the optical luminosity function as a function of absolute magnitude corrected for Galactic extinction,  $M_{B_T}$ , as given in Ho et al. (1997a). Note that Ho & Ulvestad (2001) tabulated absolute magnitudes that were corrected for both Galactic *and* internal extinction,  $M_{B_T}^0$ ; here, we do not apply the correction for internal extinction, in order to facilitate comparison with other samples. Figure 2 compares our luminosity function to the result for the CfA Seyferts, adapted from Huchra & Burg (1992). The optical magnitudes of the CfA Seyferts were not corrected for Galactic extinction, but this correction is expected to be small at the high Galactic latitudes of that sample. We stress that the optical luminosity functions pertain to the *integrated* light of the whole galaxy (nucleus plus host), rather than just the active nucleus alone, which can be significantly fainter (Ho & Peng 2001).

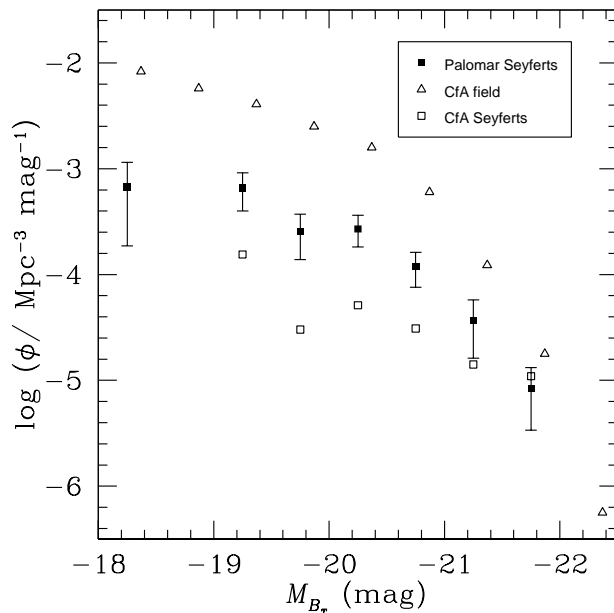


FIG. 2.— Optical luminosity function of Palomar Seyferts, compared to CfA Seyferts and CfA field galaxies. The CfA data are from Huchra & Burg (1992), converted to  $H_0 = 75 \text{ km s}^{-1} \text{ Mpc}^{-1}$ . To reduce clutter, error bars have been plotted only for the Palomar Seyferts. Only bins containing more than one galaxy have been plotted.

From the data shown in Figure 2, it is evident that the derived luminosity function for the Palomar Seyferts is a factor of 5–10 higher than the CfA Seyferts for  $-22 \text{ mag} \leq M_{B_T} \leq -19 \text{ mag}$ . This is consistent with the fact that of the 35 galaxies in the statistical Palomar Seyfert sample that are within the selection limits of the CfA survey, only 10 were recognized as Seyferts in that survey. The derived luminosity function also shows that the space density of Palomar Seyferts may approach that of the field galaxies in the CfA sample near  $M_{B_T} \approx -22 \text{ mag}$ , implying that a large fraction of galaxies of this total luminosity host at

least a weak Seyfert nucleus.

### 3.4. Radio Luminosities

#### 3.4.1. Seyfert 1 vs. Seyfert 2 Galaxies

Over the years, many studies have been made of the radio luminosities of Seyfert galaxies, and the relation to Seyfert type. Early studies generally indicated that Seyfert 2 galaxies are more luminous radio sources than Seyfert 1 galaxies at centimeter wavelengths for objects obeying the same (sometimes ill-defined) selection criteria (de Bruyn & Wilson 1978; Ulvestad & Wilson 1984a,b). However, the ultraviolet selection for Markarian and other Seyfert galaxies strongly biased the early samples toward Seyfert 2 galaxies that were much higher on the radio luminosity function than the Seyfert 1 galaxies (see discussion in Ho & Ulvestad 2001, § A.2). Later papers (Edelson 1987; Ulvestad & Wilson 1989; Giuricin et al. 1990) seemed to indicate that the discrepancy between the two Seyfert types disappeared with less biased samples, although these studies also suffered from poor resolution (Edelson 1987) and from sample heterogeneity (Ulvestad & Wilson 1989; Giuricin et al. 1990). Most recently, high-resolution 3.6 cm VLA imaging has shown that Seyfert 1 and Seyfert 2 galaxies have indistinguishable radio luminosities in samples selected at  $12 \mu\text{m}$  (Thean et al. 2001) and at  $60 \mu\text{m}$  (Schmitt et al. 2001a). Therefore, a general consensus has evolved that Seyfert 1 and Seyfert 2 galaxies have statistically similar radio luminosities, a result which has served as a strong argument in favor of the unified schemes for Seyferts.

Ho & Ulvestad (2001) provided measures of the 6 and 20 cm radio luminosities of the Palomar Seyferts, both in cores unresolved by the VLA and in the total emission associated with the active nuclei. Histograms of the total radio luminosities are shown in Figure 3; these differ slightly from the plots shown by Ho & Ulvestad (2001), because we consider here the more restricted sample of 45 Seyferts. The type 1 Seyferts appear to be somewhat more luminous in the radio than the type 2 Seyferts, exactly the opposite of the early studies that showed apparent differences between the Seyfert types. For example, at 6 cm, all eight undetected objects are Seyfert 2 galaxies; at 20 cm, 13 of the 14 undetected objects are type 2 Seyferts. More quantitatively, the Gehan-Wilcoxon test gives a 2.0% probability that the 6 cm core powers of the type 1 and type 2 Seyferts would differ as much as observed if they were drawn from the same parent distribution; this probability is 1.3% for the total 6 cm emission of the two Seyfert types. At 20 cm, both the core and total radio powers appear to be correlated with Seyfert type, with a probability of only 0.9% that the Seyfert 1 and Seyfert 2 galaxies would look as different as observed if they were drawn from the same parent population.

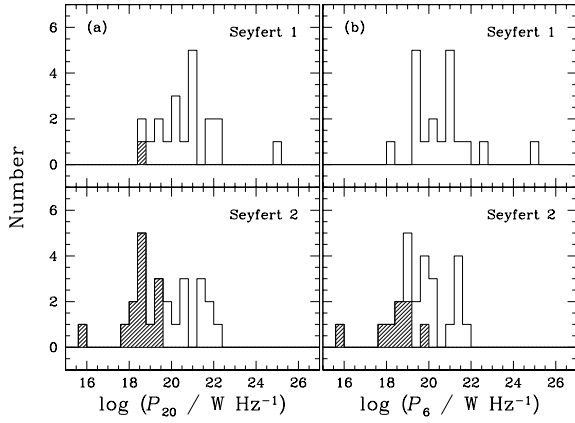


FIG. 3.— Histogram of (a) the total 20 cm radio powers and (b) the total 6 cm radio powers for the galaxies in the Palomar Seyfert sample. Upper limits are shown hatched.

These results would appear to swing the pendulum back in the direction of there being intrinsic differences between the radio luminosities of Seyfert 1 and Seyfert 2 galaxies, with the Seyfert 1 galaxies being stronger rather than weaker. Of course, any bias toward more powerful Seyfert 1 galaxies being selected from the Palomar galaxy survey also could account for the apparent differences. The effect is not due to distance; as noted in § 3.1, the Seyfert 1 galaxies are, in fact, slightly closer (on average) than the Seyfert 2 galaxies in our sample. Further discussion on this unexpected result is deferred to § 4.3 and 4.4.

### 3.4.2. Radio Luminosity Functions

Radio luminosity functions can be derived for our optically selected sample by first finding the bivariate optical-radio luminosity function, and then using that to derive the radio luminosity function, as was done by Meurs & Wilson (1984). We have carried out this procedure for both the 6 and 20 cm observations, computing the luminosity functions down to values below which more than 75% of the measurements are upper limits. Extending the analysis to lower luminosities would be subject to large uncertainties, due to the fact that very few detections are present in the same luminosity range as most of the upper limits. At 6 cm, where the upper limit for NGC 5395 fell well above many detections, this limit has been distributed among the lower bins according to the population of sources in those bins. However, since  $V_{\max}$  is quite high for NGC 5395, this galaxy has relatively low weight and does not affect the results appreciably.

Table 2 lists both the 6 and 20 cm luminosity functions. Figure 4a shows the 20 cm luminosity function compared to results from other samples (most of which were derived at 20 cm), while the 6 cm luminosity function for the Palomar Seyferts is in Figure 4b. We make no effort to distinguish between the two Seyfert types, because each of the samples contains  $\lesssim 50$  galaxies, insufficient to populate most of the luminosity bins adequately for each type. In Figure 4a, the 20 cm luminosity functions found by Meurs & Wilson (1984) for the Markarian Seyferts and by Ulvestad & Wilson (1989) for a distance-limited Seyfert sample have been converted to our adopted value of  $H_0 = 75 \text{ km s}^{-1} \text{ Mpc}^{-1}$ .

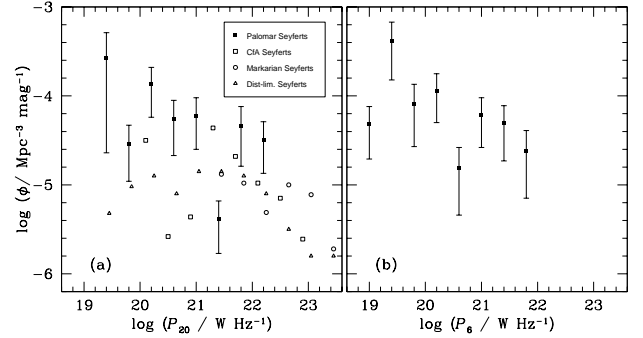


FIG. 4.— Radio luminosity functions of Palomar Seyferts at (a) 20 cm and (b) 6 cm. Only bins containing more than one galaxy have been plotted. Panel (a) also shows data for the Markarian Seyferts (Meurs & Wilson 1984), distance-limited Seyferts (Ulvestad & Wilson 1984b, 1989) and CfA Seyferts (Kukula et al. 1995). The luminosities of the CfA Seyferts have been converted from 3.6 cm to 20 cm using a spectral index of  $\alpha = -0.7$ , and their points are offset to the left by 0.1 in  $\log P_{20}$  for clarity.

Kukula et al. (1995) did not present a radio luminosity function for the CfA Seyferts. We have converted their C-configuration 3.6 cm flux densities to 20 cm using a spectral index of  $-0.7$ , and then computed the luminosity function using the  $V/V_{\max}$  technique. We used their low-resolution ( $2''$ ) flux densities rather than the values at  $0''.25$  resolution because the angular scale sampled is more comparable to the total flux densities used for the Palomar Seyfert sample. As a check, we compared the 20 cm flux densities estimated in this way to those measured by us for nine galaxies in common between the CfA and Palomar samples. The mean difference is  $\langle \log(P_{\text{CfA}}) - \log(P_{\text{Pal}}) \rangle = 0.09$  dex, with an rms scatter of 0.25 dex. Except for NGC 4235, which actually is known to have a much flatter spectrum than the assumed value of  $-0.7$  (Ulvestad & Wilson 1989), the remaining eight galaxies all have 20 cm powers extrapolated from the Kukula et al. (1995) measurements that are within 0.25 dex of those measured directly by Ho & Ulvestad (2001).

Figure 4a shows that the radio luminosity functions for the Palomar, CfA, distance-limited, and Markarian samples are consistent with one another for  $P_{20} \gtrsim 10^{21} \text{ W Hz}^{-1}$ , given the small numbers of galaxies present. It appears that the Palomar Seyferts have significantly higher space densities at radio luminosities below  $\sim 10^{21} \text{ W Hz}^{-1}$ . This is consistent with expectations, because the Palomar sample generally includes more nearby and weaker Seyferts than the other three samples, which are undoubtedly incomplete at the lower power levels. Indeed, the luminosity function for the Markarian sample does not even extend to values below  $P_{20} \approx 10^{21.5} \text{ W Hz}^{-1}$ .

### 3.5. Correlations between Radio and Optical Emission Lines

Strong correlations of 20 cm continuum power with [O III]  $\lambda 5007$  emission-line luminosity and line width have been well established for Seyferts (de Bruyn & Wilson 1978; Wilson & Willis 1980; Heckman et al. 1981; Meurs & Wilson 1984; Whittle 1985); the basic results were summarized by Wilson (1991). Whittle (1985) showed that the relationship between radio power and line luminosity appears to hold over several orders of magnitude in each variable. Whittle (1992a, 1992b) later showed that the relation between radio luminosity and [O III] line width indicates anomalously large widths in pow-

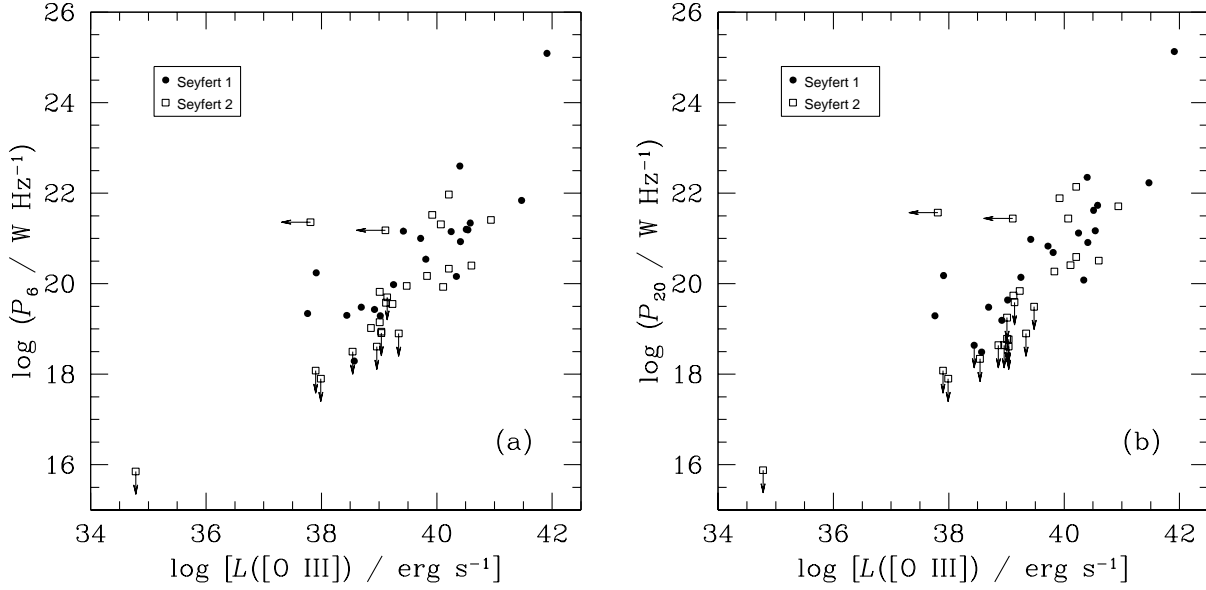


FIG. 5.— Plots of (a) 6 cm radio power and (b) 20 cm radio power vs. the extinction-corrected [O III] luminosity for Palomar Seyferts. Seyfert 1 and 2 galaxies are distinguished by closed and open symbols, respectively.

erful linear radio sources ( $P_{20} > 10^{22} - 10^{23} \text{ W Hz}^{-1}$ ), which appear to accelerate narrow-line gas beyond the values expected for virialized motions. However, the correlation still held for galaxies with weaker radio sources, indicating a remaining relationship with bulge luminosity. For Seyfert 1 galaxies, radio-quiet and radio-loud objects cover the same range of [O III] luminosities, but Ho & Peng (2001) have shown that the correlation of radio power with [O III] line luminosity actually has two distinct relations, one for radio-quiet and one for radio-loud objects (where “radio-loud” and “radio-quiet” are defined by using the radio-to-optical luminosity ratio of the active nucleus, rather than of the entire galaxy).

Not surprisingly, computation of the generalized Kendall’s  $\tau$  coefficient for the Palomar Seyfert sample shows that both the 20 and 6 cm radio powers are correlated with the [O III] luminosity<sup>1</sup>, with the probability of a null correlation being less than 0.01%. Plots of these relationships are shown in Figure 5. A similar relationship is obtained by plotting the radio fluxes against emission-line fluxes (not shown, to save space), so the apparent correlation is not just a distance effect. The actual values of radio power at a given [O III] strength are scattered over more than two orders of magnitude. For example, at 6 cm, Figure 5a shows that the radio power varies from  $\sim 10^{20}$  to  $\sim 10^{22} \text{ W Hz}^{-1}$  at an [O III] line luminosity near  $10^{40} \text{ erg s}^{-1}$ . Testing the correlation of [O III] luminosity alone against Seyfert type, we find a 15% probability that the different Seyfert types would look as different as observed if drawn from the same parent population in [O III] luminosity.

Previously, there were indications from the heterogeneous sample of objects studied by Whittle (1985) that Seyfert 2 galaxies have higher radio powers (by a factor of 5–10) than Seyfert 1 galaxies at a given [O III] luminosity. We can test to see whether the ratio of radio power to [O III] luminosity is

the same for the two Seyfert types. In this case, the generalized Kendall’s  $\tau$  coefficient shows that the ratio of total 20 cm power to [O III] luminosity is significantly different between Seyfert 1 and Seyfert 2 galaxies; if the two Seyfert types were drawn from the same parent population, the observed difference would be expected only 0.9% of the time. Using the 6 cm power instead, the difference is significant at the level of 1.2%. The apparent correlation is in the sense that, for a given [O III] luminosity, the radio power is *higher* for Seyfert 1 galaxies than for Seyfert 2 galaxies, opposite to the sense suggested by Whittle (1985).

Along with the tests of radio vs. optical emission-line strength, we have tested for correlation of the radio powers at both 6 and 20 cm with the kinematics of the narrow-line region. This test traditionally makes use of the [O III]  $\lambda 5007$  line (Wilson & Willis 1980; Whittle 1985, 1992a). For the Palomar survey, however, the red spectral region has higher dispersion than the blue spectral region, and Ho et al. (1997a) use the [N II]  $\lambda 6584$  line as a surrogate for [O III]  $\lambda 5007$  to quantify the width of the narrow emission lines. In the narrow-line regions of Seyfert galaxies, [N II] and [O III] trace roughly similar kinematics (e.g., Busko & Steiner 1992). We use the values of  $\text{FWHM}([\text{N II}])$  as given in Ho & Ulvestad (2001), but omit NGC 777, for which [N II] was not detected. In this case, we again find a highly significant correlation, with the probability of no correlation being less than 0.01% for both radio frequencies. Scatter plots are shown in Figure 6. As for the plots of radio power vs. [O III] luminosity, a scatter of two orders of magnitude or more in the radio power is seen for a given value of the [N II] line width. Few of the Palomar Seyferts have 20 cm radio powers above  $10^{22} \text{ W Hz}^{-1}$ , so we would expect few of the outliers with high line width that were identified in strong linear radio sources by Whittle (1992a). In fact, the one galaxy

<sup>1</sup> In this and subsequent discussions, the [O III] luminosity pertains to the  $\lambda 5007$  line, corrected for Galactic and internal extinction, as described in Ho et al. (1997a).

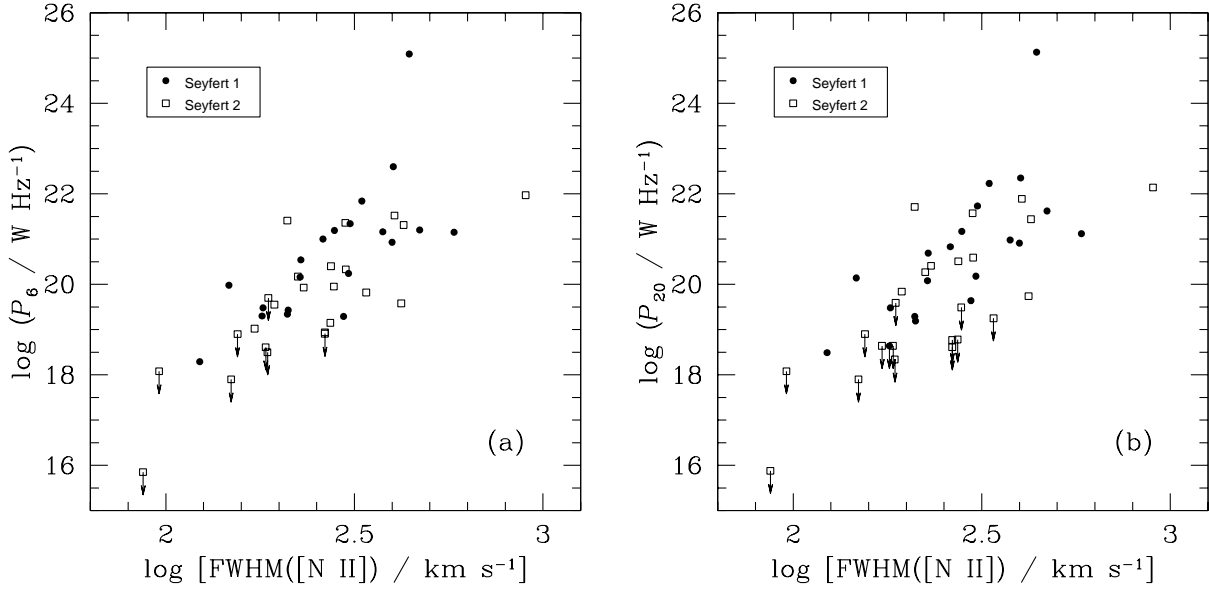


FIG. 6.— Plots of (a) 6 cm radio power and (b) 20 cm radio power vs. [N II] line width for Palomar Seyferts. Seyfert 1 and 2 galaxies are distinguished by closed and open symbols, respectively.

with a strong radio power and an anomalously high line width is NGC 3079 ( $\log P_6 = 21.97$ ,  $\log P_{20} = 22.14$ ,  $\text{FWHM}([\text{N II}]) = 900 \text{ km s}^{-1}$ ), which appears to be dominated by a diffuse radio source rather than a linear source (Ho & Ulvestad 2001).

### 3.6. Radio Spectra

Most previous Seyfert samples observed at radio wavelengths do not have high-resolution, multi-frequency spectral information. An exception is the distance-limited sample of Ulvestad & Wilson (1984b, 1989), which includes arcsecond imaging at 6 and 20 cm for a total of 43 galaxies. Only two of those 43 galaxies have “flat” radio spectra, where “flat” spectra are defined to have spectral indices  $\alpha \geq -0.2$  (using the definition that  $S_\nu \propto \nu^{+\alpha}$ ). The distribution of spectral indices from this distance-limited sample is shown in Figure 7. However, a cautionary note is that the distance-limited sample was observed at higher resolution at 6 cm than at 20 cm, so there could be a tendency for the total fluxes at 6 cm to be underestimated relative to 20 cm. This might yield steeper spectra than observations with matched beam sizes, as was achieved with the Palomar sample.

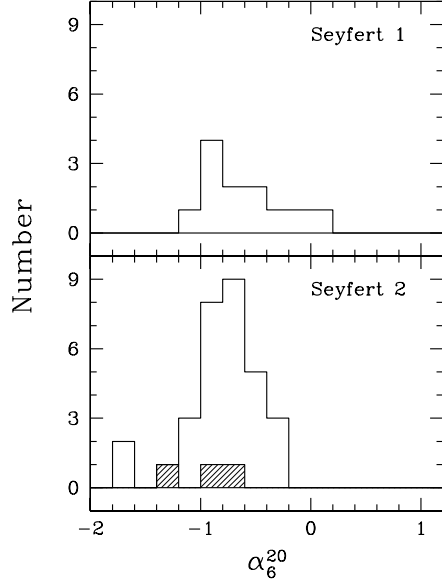


FIG. 7.— Histogram of two-point spectral indices between 20 and 6 cm for the distance-limited Seyfert sample of Ulvestad & Wilson (1984b, 1989). Upper limits (detections at 20 cm and upper limits at 6 cm) are indicated by hatched regions.

Ho & Ulvestad (2001) gave two-point radio spectral indices for the galaxies in the Palomar Seyfert sample that were detected at both 6 and 20 cm. We have added to these values the limits for the objects that were detected only at 6 cm. In addition, in order to isolate any core component which may potentially lie within the region of the torus, we have computed the spectral indices from the peak emission at the highest resolution, with similar  $(u, v)$  coverage and identical restoring beams at 6 and 20 cm. Figure 8 shows histograms of the spectral in-

dices of the peak and total radio emission for the 37 galaxies in the statistical sample that were detected at 6 cm and/or 20 cm. Fifteen of these galaxies have total spectral indices of  $\alpha \geq -0.2$ , while 19 have spectral indices of their peaks falling in the same range.

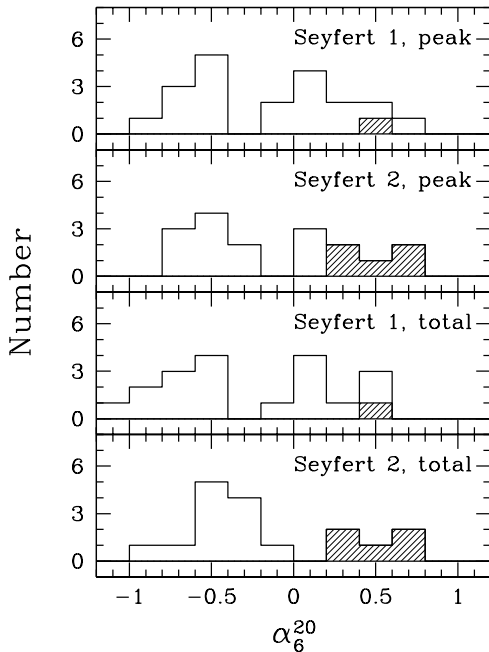


FIG. 8.— Histogram of two-point spectral indices between 20 and 6 cm for the Palomar Seyfert galaxies. Lower limits (detections at 6 cm and upper limits at 20 cm) are indicated by hatched regions.

There is a clear difference between the Palomar sample and the distance-limited sample of Ulvestad & Wilson (1984b, 1989), with a probability of less than 0.01% that the two distributions would differ by the observed amount if drawn from the same parent population (even though a few galaxies are in both samples). Given the large number of objects in both samples that are unresolved or slightly resolved, we do not expect possible resolution effects in the distance-limited sample to account for the dramatic differences in spectral indices. For example, if we consider only those sources that were unresolved in the distance-limited sample, only 18% (2 of 11) have  $\alpha \geq -0.2$ , substantially fewer than the 41% (15 of 37) Palomar Seyferts with similarly flat spectra.

There is a slight indication from Figure 8 that Seyfert 2 galaxies have systematically larger (i.e., flatter or more inverted) radio spectral indices than Seyfert 1 galaxies. Certainly, most of the sources with lower limits to their spectral indices are Seyfert 2 galaxies. However, the differences are not statistically significant. The Gehan-Wilcoxon test gives a 29% probability that the total spectral indices of the two Seyfert types would differ by the observed amount if drawn from the same parent population, or a 63% probability using the spectral indices of the peaks.

### 3.7. Radio Source Sizes

Early suggestions were that Seyfert 2 galaxies were not only more powerful than Seyfert 1 galaxies at centimeter wavelengths, but also had larger radio sources (Ulvestad & Wilson 1984a,b). After controlling for the strengths of the radio sources by measuring sizes at a uniform fraction of the

radio peak, Ulvestad & Wilson (1989) found that this difference was not statistically significant. However, in the unified schemes, one would expect the Seyfert 1 galaxies to have generally smaller radio sources. Since Seyfert 1 galaxies would have more nearly face-on tori, their radio jets would be expected to lie along the line of sight to the observer, and hence be foreshortened. Indeed, Schmitt et al. (2001a) have found just this effect in the de Grijp et al. (1992) sample of Seyfert galaxies selected at 60  $\mu$ m.

Figure 9 shows the distribution of radio sizes for the active-nucleus components of the Seyfert galaxies in the Palomar sample. Making a statistical study of the radio sizes of these galaxies is subject to considerable uncertainty; some radio sources are unresolved, while others are undetected. Therefore, we have performed the Gehan-Wilcoxon test on two different subsamples of Seyfert galaxies, those with measured sizes only (19 galaxies), and those with either measured sizes or upper limits (37 galaxies). These tests show respective probabilities of 74% and 31% that the two Seyfert types would differ by the observed amount if they were drawn from the same parent population. The contradiction with Schmitt et al. (2001a), who found the Seyfert 1 radio sources to be smaller than the Seyfert 2 sources in the 60- $\mu$ m sample, may be due to our larger beam size (by an areal factor of 25 for full-resolution maps, and more than 100 for tapered maps). This provides considerably higher sensitivity to low-surface-brightness emission that is not necessarily jet-related, and might not have been detected in the high-resolution 3.6 cm study of the 60- $\mu$ m sample. There also is some possibility (see § 4.3) that the Seyfert 1 galaxies in the Palomar sample are selected from higher on the luminosity function. This could cause a bias toward larger Seyfert 1 radio sources, if radio sizes are correlated with radio power, as reported in some previous work (Ulvestad & Wilson 1984b).

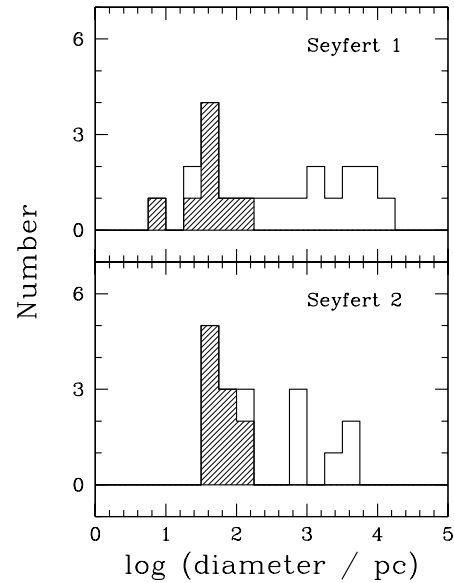


FIG. 9.— Histogram of radio sizes for the Palomar Seyfert sample, for the emission inferred to be associated with the active nucleus. Upper limits are shown hatched.

### 3.8. Radio Morphology

The radio morphologies of the Palomar Seyferts were classified by Ho & Ulvestad (2001) according to the scheme in-

troduced by Ulvestad & Wilson (1984a). Eleven of the 37 detected sources from the statistical sample of 45 galaxies contain linear radio sources (class "L"), while 18 are only unresolved or slightly resolved (classes "U" and "S," respectively). An additional six galaxies were classified as having ambiguous (class "A") structures by Ho & Ulvestad (2001), but all of these sources are barely detected, and the detected components are poorly resolved. The fraction of linear radio sources (11 of 45, or 24%) can be compared with other samples of comparable size. In the heterogeneous distance-limited sample of Ulvestad & Wilson (1984b, 1989), 13 of 57 galaxies (55 detected) have linear radio sources, while 20 of 107 galaxies in the 12- $\mu\text{m}$  sample (Thean et al. 2001) have linear sources. This indicates that about 20% to 30% of Seyfert galaxies contain linear radio sources detectable by current connected-element interferometers. However, measurements of radio morphologies and sizes may be biased by the fact that the dynamic range on the weakest galaxies is too low to see the full extent of the radio emission (Ulvestad & Wilson 1989; Thean et al. 2001). Indeed, Thean et al. (2001) find that the fraction of linear sources in the 12- $\mu\text{m}$  sample rises from 18% to 28% when only the galaxies with 3.6 cm flux densities above 5 mJy are considered.

Another way of assessing the true fraction of linear sources is to see whether the apparent radio morphologies are correlated with radio power. If we take the 11 galaxies in the Palomar statistical sample that are classified as linear *vs.* the 18 objects that are either slightly resolved or unresolved, a Gehan-Wilcoxon test shows only that the two sets of objects differ in 6 cm radio luminosity at the 8.8% significance level. If we then add the six sources classified as ambiguous by Ho & Ulvestad (2001) to the poorly resolved class (more consistent with previous work), distributions drawn from the same parent population would differ by the observed amount only 1.4% of the time. This result indicates that discussions of Seyfert radio morphologies should be carried out with caution, since it may well be that the weaker radio sources also are linear, but are so weak that the extended emission has not been detected. This possibility could be tested with observations that are 10 times more sensitive, such as those that could be made with the proposed Expanded Very Large Array (Perley 2000).

A final test of interest is to compare the radio morphologies to the Seyfert types. According to the unified scheme, where the Seyfert 1 radio sources would be seen more end-on, more linear radio sources might be distinguishable in Seyfert 2 galaxies. In § 3.7, it was shown that there was no significant correlation between radio size and Seyfert type for the Palomar sample. The Gehan-Wilcoxon test shows that for the galaxies classified as linear *vs.* the slightly resolved or unresolved galaxies, the morphological classes for the two Seyfert types would differ by the observed amount 9.2% of the time if they were drawn from the same parent sample. However, this probability shrinks to 2.9% if the six ambiguous objects are included with the poorly resolved sources. The difference in the Palomar sample is in the sense that the Seyfert 1 galaxies have a *higher* probability of containing linear radio sources than the Seyfert 2 galaxies, opposite to what might be expected if the Seyfert 1 radio sources are seen more end-on. However, for the small number of linear sources in the sample, and given a possible tendency to identify stronger Seyfert 1 galaxies (see § 4.3), this result requires verification in a larger sample.

### 3.9. Radio Axes vs. Galaxy Axes

Seyfert galaxy radio sources are thought to be powered by radio jets which emerge from the vicinity of a supermassive black hole, in a direction perpendicular to a circumnuclear torus. If the gas in that torus is accreted from the large-scale disk of the host galaxy, it should share the host's angular momentum axis. Therefore, one might expect the radio jets to appear predominantly perpendicular to the plane of the host galaxy. An early study (Ulvestad & Wilson 1984b) indicated that there was no excess of Seyferts with jets perpendicular to the host disks; this study was extended and confirmed by later work on larger samples, which also took account of the effects of projection of jets and galaxies on the sky (Schmitt et al. 1997; Nagar & Wilson 1999; Kinney et al. 2000).

In the Palomar Seyfert sample, there are 15 galaxies having measurable radio major axes (Ho & Ulvestad 2001). Figure 10 shows a histogram of the position angle difference between the radio and host galaxy major axes of these 15 galaxies. Clearly, the distribution is consistent with being uniform. As discussed by (Kinney et al. (2000), this is expected in a situation in which the radio jets are oriented completely randomly with respect to the host galaxies. If the radio jets are perpendicular to the central accretion disk or torus, this result implies that the disk/torus does not share the angular momentum axis of the host galaxy, perhaps implying an external origin for the accreting gas. More detailed discussion of possible reasons for the observed distribution of position angle differences can be found in Kinney et al. (2000).

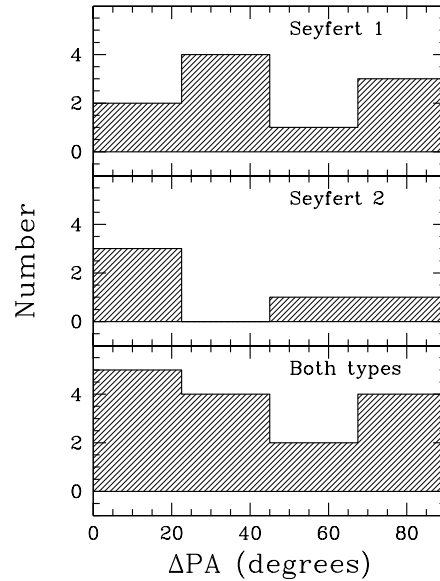


FIG. 10.— Histogram of the difference between the position angle of the radio and host galaxy major axes for 15 well resolved objects in the Palomar Seyfert sample. The radio axis is from the emission inferred to be associated with the active nucleus, rather than with the large-scale galaxy.

## 4. ADDITIONAL INTERPRETATION

A considerable amount of discussion about the various statistical correlations in Seyferts has been carried out in § 3. The physical meaning of various correlations has been explored at length recently by Thean et al. (2001) for the 12- $\mu\text{m}$  Seyfert sample, and by (Schmitt et al. 2001a) for the 60- $\mu\text{m}$  Seyfert sample; we do not propose to conduct a similar exhaustive discussion for the Palomar Seyferts. Instead, we limit ourselves to

some general points, and a more detailed exploration of some of the results that appear unique to the Palomar sample.

First, we summarize the results of our statistical tests in Table 3. For each test described in § 3, the statistical significance of that test is given, along with a reference to the relevant subsection. For completeness, the table also includes a few additional tests that are discussed below. Customarily, the results of statistical tests are deemed significant if the null hypothesis can be rejected at a probability of 5% or less. In Table 4, we list the primary arcsecond-resolution surveys of various Seyfert samples. Statistical results for these samples are of interest for comparison with the Palomar Seyferts, and will occasionally be cited below.

#### 4.1. The Space Density of Weak Seyfert Galaxies

The optical luminosity function given in Table 1 can be integrated to find the total space density of weak Seyfert galaxies, such as those which dominate the Palomar sample. In the range of  $-22 \text{ mag} \leq M_{B_T} \leq -18 \text{ mag}$ , the space density of Palomar Seyferts is  $(1.25 \pm 0.38) \times 10^{-3} \text{ Mpc}^{-3}$ . By comparison, we can look at the local space density of bright quasars, as derived by Hewett, Foltz, & Chaffee (1995). In the range  $0.2 < z < 0.5$  (after conversion to our Hubble constant), they find space densities for bright quasars of  $\sim 5 \times 10^{-6} \text{ Mpc}^{-3}$ , or  $\sim 1.4 \times 10^{-6} \text{ Mpc}^{-3}$  after the objects with Seyfert galaxy luminosities are eliminated. Thus, the local space density of weak Seyferts appears to be  $\sim 700$  times higher than the local space density of bright quasars.

As a consistency check, we also can compare the Seyfert results to the overall space density of galaxies in the Palomar galaxy survey. First, we eliminate the galaxies having southern declinations or apparent magnitudes  $B_T > 12.64 \text{ mag}$ , which reduces the initial sample of 486 galaxies (Ho et al. 1995) to a statistical sample of 435 galaxies. Computation of the space density of bright galaxies then follows the  $V/V_{\max}$  method. We find that the total space density of bright galaxies is  $(3.0 \pm 1.2) \times 10^{-1} \text{ Mpc}^{-3}$ . This density is dominated by intrinsically faint, nearby galaxies. Using only the 392 galaxies with absolute magnitudes of  $-22 \text{ mag} \leq M_{B_T} \leq -18 \text{ mag}$ , where the density of Seyfert galaxies was derived, we find a cumulative space density of  $(1.30 \pm 0.11) \times 10^{-2} \text{ Mpc}^{-3}$  for the Palomar bright galaxies. This is in good agreement with the value found for the RSA spirals by Condon (1989), after conversion to our distance scale. Thus, Seyferts comprise  $9.6\% \pm 3.0\%$  of the space density of nearby galaxies brighter than  $M_{B_T} = -18 \text{ mag}$ , as expected from the fact that 45 of the 392 objects (11.5%) above this optical luminosity are members of our statistical Seyfert sample. We also can compare the space density of Palomar Seyferts to that of the CfA Seyferts (Huchra & Burg 1992), after conversion to our distance scale. The derived CfA Seyfert space density in the range  $-22 \text{ mag} \leq M_{B_T} \leq -18 \text{ mag}$  is  $(1.47 \pm 0.39) \times 10^{-4} \text{ Mpc}^{-3}$ . Formally, the ratio of the CfA Seyfert density to the Palomar Seyfert density is then  $0.12 \pm 0.05$ . The overall galaxy density in the CfA sample is  $\sim 1.1 \times 10^{-2} \text{ Mpc}^{-3}$  in the same absolute magnitude range (comparable to the RSA value found above), so the fraction of galaxies detected as Seyferts in the CfA survey is only  $\sim 1\%$ . This indicates, as discussed by Ho & Ulvestad (2001), that the CfA survey identified only a small fraction of the galaxies containing weak Seyfert characteristics in their optical spectra.

#### 4.2. Emission-Line Correlations

For all the Seyfert samples observed at arcsecond resolution, and tested statistically, the radio source powers are strongly correlated with the strengths and widths of the narrow optical emission lines. Whittle (1992a, 1992b) has made a detailed study of the origin of these correlations. He found that most Seyfert galaxies have emission-line widths that are virialized in the bulge potential of the host galaxy. However, the Seyferts with more powerful linear radio sources have “extra” line width, which can be attributed to interaction between the line-emitting gas and the moderately strong radio jets in these objects. The latter interpretation is supported by comparison of Seyferts with linear radio morphologies to high-resolution emission-line imaging of the same objects; the radio sources and emission lines have similar angular extents and are roughly aligned along the same position angles (Whittle et al. 1986; Wilson & Tsvetanov 1994; Bower et al. 1995; Capetti, Axon, & Macchetto 1997; Falcke, Wilson, & Simpson 1998). This spatial relationship could be due to interactions between the emission-line clouds and the radio plasma, although one also might expect such a result based on collimation of the radio jets and generation of a photoionization cone by the same accretion disk or torus. A detailed study by Bicknell et al. (1998) indicates that the narrow-line region might be completely powered by the radio jet, although this study uses as examples only several relatively high-power linear radio sources, and not the bulk of the less radio-luminous Seyferts. The overall narrow emission-line spectrum of Seyferts can be reasonably explained in the context of pure photoionization models (e.g., Ferland & Osterbrock 1986; Ho, Shields, & Filippenko 1993b). In addition, reverberation mapping of the smaller broad-line region (Peterson 1993; Wandel, Peterson, & Malkan 1999; Peterson & Wandel 2000) strongly favors the standard photoionization paradigm with an ionizing continuum similar to that invoked to account for the narrow lines.

For a given optical line strength or width, the radio power of the Palomar Seyferts may range over two orders of magnitude or more, as shown in § 3.5. This suggests that the emission lines and radio-emitting plasma may not be directly related, but are instead controlled by some third governing factor, such as the properties of the nuclear bulge (Whittle 1992a, 1992b). Recent work by Evans et al. (1999) indicates that the ionization of the gas does not seem to be strongly influenced by pre-ionization from the radio jet in Seyfert galaxies, so the jet appears to be coupled only loosely to the line-emitting gas.

In the Palomar Seyfert sample, we find that the *ratio* of radio power to [O III] luminosity is significantly correlated with Seyfert type: it is higher in Seyfert 1 galaxies than in Seyfert 2 galaxies (see § 3.5). Careful inspection of Figure 5 shows that this difference may be strongly influenced by the low-luminosity objects; the Seyfert 1 and Seyfert 2 galaxies appear to be well mixed within those objects having [O III] luminosities above  $L(\text{[O III]}) = 10^{39.5} \text{ erg s}^{-1}$ , while the Seyfert 2 galaxies seem to have systematically weaker radio sources for lower  $L(\text{[O III]})$ . Accordingly, we have divided the galaxies into two samples, those with  $L(\text{[O III]})$  above and below  $10^{39.5} \text{ erg s}^{-1}$ . Application of the Gehan-Wilcoxon test to these two samples shows that there is no significant correlation of the radio/[O III] ratio with Seyfert type among the galaxies with the high values of  $L(\text{[O III]})$ ; probabilities that the two Seyfert types would differ by as much as observed if they were drawn from the same parent sample are 51% for the 20 cm power and 26% for the 6 cm power. However, for the weaker objects, the similar prob-

abilities are only 1.3% at 20 cm and 3.1% at 6 cm.

The differences between Seyfert 1 and Seyfert 2 galaxies among the objects with low emission-line luminosities would be even more significant were it not for two galaxies with high radio powers and only upper limits to their [O III] emission, shown most clearly in the upper left of Figure 5b. It turns out that these two objects are NGC 777 and NGC 4472, two of the four elliptical galaxies in our statistical sample. It is conceivable that the radio-[O III] relation depends on the circumnuclear environment of the host, which might differ between elliptical and spiral galaxies. If we remove all four elliptical galaxies from the sample, the probabilities that the low-luminosity Seyfert 1 and Seyfert 2 galaxies would differ by the observed amount if drawn from the same parent population are only 0.1% at 20 cm and 0.6% at 6 cm. The median value of  $\log [P_{20} (\text{W Hz}^{-1})/L(\text{[O III]}) (\text{erg s}^{-1})]$  is -19.1 for Seyfert 1 galaxies and -20.3 for Seyfert 2 galaxies; these were calculated using the Kaplan-Meier product-limit estimator (Feigelson & Nelson 1985) to take into account the upper limits.

A test for the possible influence of starbursts is to see whether the weak Seyfert 2 galaxies follow the rather tight empirical correlation between 20 cm radio flux density and *IRAS* far-infrared flux (Helou, Soifer, & Rowan-Robinson 1985; Condon, Anderson, & Helou 1991; Condon 1992). The parameter  $q$ , which describes this ratio, is defined (Helou et al. 1985) as

$$q \equiv \log \left( \frac{FIR}{3.75 \times 10^{-12} \text{ W m}^{-2}} \right) - \log \left( \frac{S_{20}}{\text{Jy}} \right), \quad (1)$$

where

$$FIR \equiv 1.26 \times 10^{-14} \left( \frac{2.58S_{60\mu\text{m}} + S_{100\mu\text{m}}}{\text{Jy}} \right) \text{W m}^{-2}; \quad (2)$$

$S_{20}$ ,  $S_{60\mu\text{m}}$ , and  $S_{100\mu\text{m}}$  are the flux densities at 20 cm, 60  $\mu\text{m}$ , and 100  $\mu\text{m}$ , respectively. For starburst galaxies,  $q$  typically takes on the values  $2.3 \pm 0.2$ .

In the Palomar Seyfert statistical sample, 43 of the 45 galaxies have measured [O III] luminosities and values or limits to  $q$ , based on *IRAS* flux densities given in Ho et al. (1997a); these quantities are plotted against one another in Figure 11. There is an obvious inverse correlation between  $q$  and  $L(\text{[O III]})$ , which is expected since the definition of  $q$  involves radio luminosity, known to be strongly correlated with  $L(\text{[O III]})$  (Fig. 5); computation of the generalized Kendall's  $\tau$  coefficient shows that this correlation is significant at the 0.01% level. In addition, Kendall's  $\tau$  shows that  $q$  is correlated with Seyfert type, with only a 1.3% probability that the Seyfert 1 and Seyfert 2 galaxies are drawn from the same parent population. An important point to note from Figure 11 is that the Seyfert 2 galaxies with less luminous emission lines [ $L(\text{[O III]}) < 10^{39.5} \text{ erg s}^{-1}$ ] almost all have  $q \geq 1.8$  and have no detections at 20 cm. Thus, the infrared strengths of the low-luminosity Seyfert 2 galaxies are consistent with the possibility that much of their infrared and (undetected) 20 cm radio emission are due to starbursts. This is not a unique conclusion; for example, it also appears that radio-quiet quasars follow a similar radio-infrared relation to starbursts, but that the similarity could be entirely coincidental (Sanders et al. 1989).

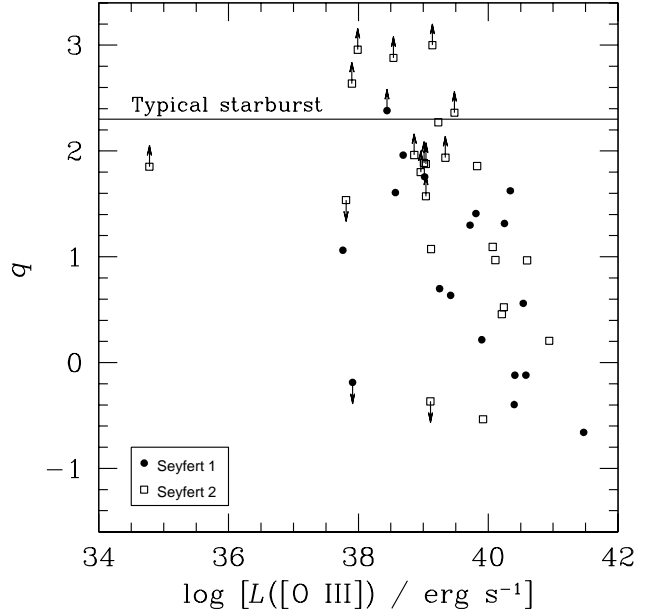


FIG. 11.— Plot of  $q$ , the logarithmic ratio of far-infrared flux to 20 cm flux density (defined in text), vs. the extinction-corrected [O III] luminosity, for the Palomar Seyfert sample.

Another way to consider whether star formation can account for the properties of the weaker Seyfert 2 galaxies is to compare in greater detail their relative emission-line strengths. If, for instance, the low- $L(\text{[O III]})$  objects are systematically contaminated by emission from H II regions, we would expect them to exhibit, on average, weaker low-ionization forbidden lines of [O I]  $\lambda\lambda 6300, 6364$ , [N II]  $\lambda\lambda 6548, 6583$ , and [S II]  $\lambda\lambda 6716, 6731$ , compared to high- $L(\text{[O III]})$  objects, since O-star photoionization generates characteristically weak low-ionization lines (Veilleux & Osterbrock 1987; Ho, Filippenko, & Sargent 1993a). However, the diagnostic diagrams plotted in Figure 12 reveal no clear differences between the two subsets of objects.

There are several possible explanations for the anomalous weakness of the radio emission from the low-luminosity Seyfert 2 galaxies. First, the galaxies may be dominated by a starburst component. The absence of spectral differences in the optical (Fig. 12), and the low radio-[O III] ratio suggest that this is unlikely. Second, Seyfert galaxies may require a certain minimum level of nuclear activity to “turn on” their radio emission. According to the unified scheme, this would mean that Seyfert 1 galaxies with low forbidden-line luminosities would be expected to have radio emission as weak as the Seyfert 2 objects. However, at the low forbidden-line strengths, the Seyfert 2 galaxies seem to have weaker radio sources than the Seyfert 1 galaxies. Third, the weak Seyfert 2 galaxies may have their nuclear radio emission obscured in some way, a possibility that is explored further in § 4.4.

#### 4.3. Radio Correlations with Seyfert Type

For the Markarian Seyferts (de Bruyn & Wilson 1978; Ulvestad & Wilson 1984a) and the first distance-limited sample of Seyferts (Ulvestad & Wilson 1984b), it appeared that type 2 Seyferts were stronger radio sources than type 1 Seyferts. However, samples that were selected more uniformly and imaged at arcsecond resolution have never shown a convincing difference in the radio powers between the two types (Ulvestad & Wilson

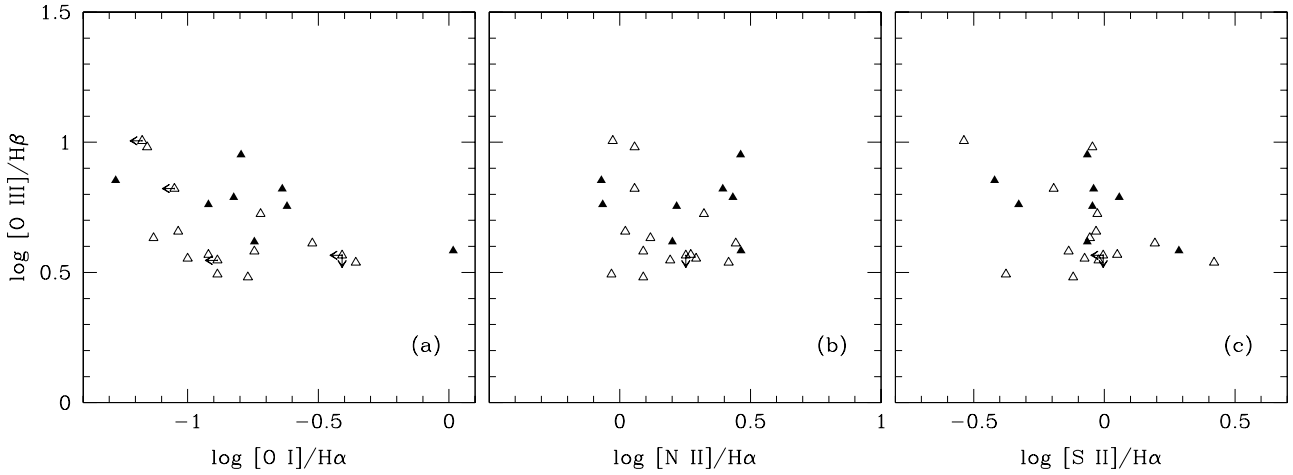


FIG. 12.— Diagnostic line-ratio diagrams for the 25 Seyfert 2 galaxies in the Palomar sample. The three panels plot the logarithmic ratios of [O III]  $\lambda 5007/\text{H}\beta$  vs. (a) [O I]  $\lambda 6300/\text{H}\alpha$ , (b) [N II]  $\lambda\lambda 6584/\text{H}\alpha$ , and (c) [S II]  $\lambda\lambda 6716, 6731/\text{H}\alpha$ . Objects with  $L([O \text{ III}]) \geq 10^{39.5} \text{ erg s}^{-1}$  and  $L([O \text{ III}]) < 10^{39.5} \text{ erg s}^{-1}$  are shown with filled and open symbols, respectively. There are no systematic differences between the two subsets of objects.

1989; Thean et al. 2001; Schmitt et al. 2001a), nor have most heterogeneous compilations of Seyferts (Giuricin et al. 1990). Thus, it came as a distinct surprise to find a statistically significant result that Seyfert 1 galaxies appear to have somewhat stronger radio sources than Seyfert 2 galaxies (see Table 3 and § 3.4.1). As discussed above (§ 4.2), this result seems to be caused by anomalously weak radio emission (for a given [O III] luminosity) in the low-luminosity Seyfert 2 galaxies.

Given the manner in which the optical classifications are made, we must consider whether subtle selection effects are inherently built into the Palomar Seyfert sample, or indeed into any sample selected by optical spectroscopy. As shown in § 3.1, there is no significant difference in the distance between the Seyfert types. However, the detection of broad emission lines, on which the distinction between type 1 and type 2 Seyferts is based, depends critically on the strength of the line emission relative to the continuum (the equivalent width), for spectra of fixed signal-to-noise ratio. This is especially true for Seyfert galaxies with intermediate types 1.8 or 1.9, which dominate the type 1 objects identified in the Palomar sample, because of the challenge in detecting the faint, low-contrast wings of the broad component of the  $\text{H}\alpha$  line (Ho et al. 1997c). All else being equal, we expect broad  $\text{H}\alpha$  to be more easily recognized in objects with higher line luminosities and higher line equivalent widths. Figure 13a indicates that the weak and strong Seyfert 2 galaxies show no distinction in their level of excitation, as characterized by the [O III]/H $\beta$  ratio. However, as shown in Figure 13b, the Seyfert 1s in the Palomar sample do indeed have higher  $\text{H}\alpha$  equivalent widths than the Seyfert 2s. The difference in line luminosity is only marginal for [O III] (Table 3), but it is more significant for  $\text{H}\alpha$  (probability of 0.8% that the two Seyfert types are drawn from the same parent population). The median extinction-corrected luminosity of the narrow-component of  $\text{H}\alpha$  is  $5.0 \times 10^{39} \text{ erg s}^{-1}$  for the Seyfert 1s, to be compared with  $1.4 \times 10^{39} \text{ erg s}^{-1}$  for the Seyfert 2s. Since radio power scales with line luminosity (Fig. 5; see discussion in Ho & Peng 2001), we naturally expect the Palomar Seyfert 1s

to be on average more radio luminous than the Seyfert 2s.

#### 4.4. The Flat-Spectrum Seyferts

In § 3.6, it was shown that a substantial fraction of the Palomar Seyferts have relatively flat radio spectra. This fraction appears considerably higher than in the distance-limited sample of Ulvestad & Wilson (1984b, 1989), even after accounting for possible resolution effects. The other samples listed in Table 4 do not have radio spectra determined at arcsecond resolution, so they cannot be usefully compared. There are several possible explanations for the flat-spectrum objects. First, the Palomar Seyferts may have objects that contain a significant fraction of their emission from supernova remnants like those in our Galaxy. Second, they may be synchrotron emitters that include self-absorbed radio cores, causing the overall spectra to be flatter than optically thin sources. Third, the emission may be “contaminated” by thermal gas, which either free-free absorbs steep-spectrum synchrotron emission, or contributes its own intrinsic emission with a nearly flat spectrum. We consider each of these possibilities in turn in the following subsections.

##### 4.4.1. Supernova Remnants

The Palomar Seyfert radio emission conceivably could arise from a collection of supernova remnants rather than from an active galactic nucleus. However, there are several strong arguments against this possibility. Collections of extragalactic supernova remnants in starbursts appear to have median spectral indices in the range between  $-0.5$  and  $-0.7$  (Lacey, Duric, & Goss 1997; Ulvestad & Antonucci 1997; Hyman et al. 2000; Neff & Ulvestad 2000), while Galactic supernova remnants have median values of  $\alpha \approx -0.45$  (Clark & Caswell 1976). A substantial number of the Palomar Seyferts have much flatter spectra, with  $\alpha \geq -0.2$  (see § 3.6). Therefore, supernova remnants do not seem able to explain the large fraction of flat spectra; if they exist in the weak Palomar Seyferts, their relatively steep spectra must be balanced by a comparable amount of flat

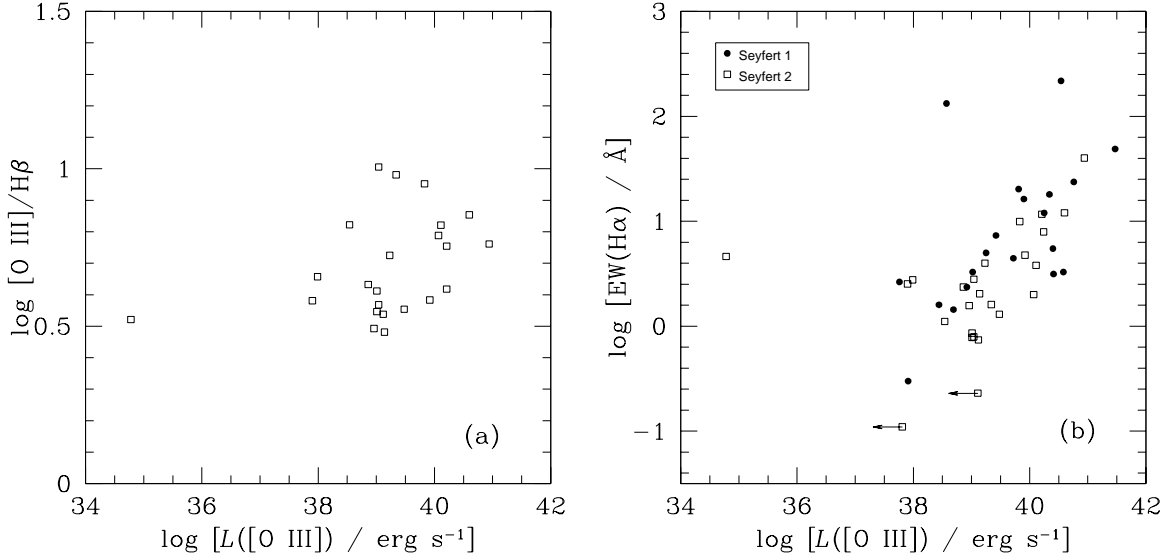


FIG. 13.— Emission-line properties plotted against the extinction-corrected [O III] luminosity for Seyfert galaxies in the Palomar sample. (a) [O III]/H $\beta$  ratio is plotted for the Seyfert 2 galaxies (two elliptical galaxies with [O III] upper limits are excluded). (b) Equivalent width of the narrow component of the H $\alpha$  emission line is plotted for all the Palomar Seyfert galaxies.

or inverted-spectrum emission from an AGN or a collection of thermal radio sources.

In addition, as shown in § 4.2, most Palomar Seyferts do not follow the nearly universal correlation between far-infrared and radio emission that is expected for galaxies undergoing active star formation. Finally, the optical spectra of these sources, by definition, do not resemble the spectra of H II regions or of supernova remnants (see, e.g., Ho et al. 1993a). Hence, the possibility that radio emission from many Palomar Seyferts is affected significantly by supernova remnants is not considered further here.

#### 4.4.2. Self-Absorbed Synchrotron Emission

If a substantial fraction of the Palomar Seyferts contain self-absorbed synchrotron sources (Williams 1963), they must have radio cores with brightness temperatures of  $\sim 6 \times 10^9$  K or greater. A number of the objects with relatively flat spectra are detected at 6 cm with flux densities of  $\sim 0.5$  mJy, and have no detection at 20 cm. For an object to have a flux density of 0.5 mJy and a brightness temperature above  $6 \times 10^9$  K at 5 GHz, its angular size must be less than about 2 mas, corresponding to a linear size of less than 0.2 pc at a typical distance of 20 Mpc. This combination of parameters is at the limit accessible by present-day VLBI systems. However, there are a few stronger flat-spectrum sources in our sample. A source such as NGC 4565, with a flux density of 2.7 mJy, would have a brightness temperature above the self-absorption limit if its size were less than about 4 mas. Such a source could be imaged using the Very Long Baseline Array (VLBA).

We note here that Falcke et al. (2000) have used VLBA observations to find a substantial population of high-brightness objects among LINERS with cores of a few mJy or higher, which would favor the possibility that the Palomar Seyferts could have similar cores. Therefore, at least one class of weak AGNs has cores compact enough that they might be self-

absorbed, lending some credence to the possibility that weak Seyferts also might have such cores. Such compact sources also would be expected to be variable. The only search for variability in a significant sample of weak AGNs was reported recently by Falcke et al. (2001), and at least some mJy-level Seyferts from the Palomar sample appear to vary at 15 GHz on time scales of years. Radio-quiet quasars with flat-spectrum cores, at similar flux levels (but higher luminosities) appear to have a high incidence of variability as well (Barvainis, Lonsdale, & Antonucci 1996). Further studies of radio variability in the Palomar sample would be useful.

The possibility of self-absorption, however, does not explain why the Palomar Seyferts have significantly flatter spectra than the distance-limited sample of Ulvestad & Wilson (1984b, 1989), in the absence of a plausible physical mechanism by which less luminous radio sources, which typify the Palomar sample, are systematically more likely to be self-absorbed. One possibility is that low-luminosity AGNs experience highly sub-Eddington accretion rates, such that their accretion undergoes an optically thin advective flow. Advection-dominated accretion flows (ADAFs; see Narayan, Mahadevan, & Quataert 1998 for a review) have been invoked to explain a number of low-luminosity galactic nuclei (e.g., Narayan, Yi, & Mahadevan 1995; Lasota et al. 1996; Quataert et al. 1999; Ho et al. 2000). Wrobel & Herrnstein (2000) have found that the low-power radio cores of some elliptical galaxies are consistent with the presence of ADAFs. ADAF models robustly predict that the self-absorbed radio spectrum should rise with frequency as  $\nu^{2/5}$  until it reaches a maximum frequency, beyond which the plasma becomes optically thin (e.g., Mahadevan 1997; Narayan et al. 1998). The observed spectral indices, therefore, could easily arise from an ADAF core component diluted (in some cases) by a steep-spectrum jet component. ADAF models predict that the spectrum should continue to rise slowly into the millimeter/sub-millimeter regime, so sensitive observations at

100 GHz or higher could provide a strong test of the viability of an ADAF model for the low-luminosity Seyferts.

#### 4.4.3. Thermal Gas

Another possibility is that enough thermal gas is present in the Palomar Seyferts to account for the flat spectra, either by free-free emission or by free-free absorption of intrinsically steeper synchrotron spectra. Low-frequency flattening in a Seyfert spectrum was first detected in NGC 1068 at wavelengths longer than 20 cm by Pedlar et al. (1983). Most of the spectra in Palomar Seyferts are not strongly inverted between 6 and 20 cm. Therefore, if free-free absorption is present, the typical galaxy is likely to have an optical depth of unity at some wavelength between 20 and 6 cm. However, there are examples such as NGC 1275 (3C 84; one of the members of our sample), whose jet is strongly free-free absorbed on parsec scales at wavelengths shorter than 6 cm (Levinson, Laor, & Vermeulen 1995; Walker et al. 2000). The situation may be considerably more complex than that for a single absorbing component; free-free absorption in Seyfert galaxies imaged with VLBI sometimes appears to occur in front of some, but not all, individual radio components (Roy et al. 1998; Ulvestad et al. 1999).

The free-free optical depth can be approximated as (Mezger & Henderson 1967)

$$\tau_{\text{ff}} \approx 8.235 \times 10^{-2} T_e^{-1.35} \nu_9^{-2.1} n_e^2 L_{\text{pc}}, \quad (3)$$

where  $T_e$  is the electron temperature in Kelvins,  $\nu_9$  is the observing frequency in GHz,  $n_e$  is the electron density in  $\text{cm}^{-3}$ , and  $L_{\text{pc}}$  is the path length in parsecs. Using this equation, and assuming the presence of ionized gas at  $T_e = 10^4$  K, we find that  $\tau_{\text{ff}} = 1$  at 2–3 GHz for an emission measure  $E \equiv n_e^2 L_{\text{pc}} = (1.3 - 3.1) \times 10^7 \text{ cm}^{-6} \text{ pc}$ .

Most of the flat-spectrum radio sources among the Palomar Seyferts are dominated by an unresolved component, with a typical size upper limit of 100 pc or less (see Fig. 9). As an illustrative example, we consider the Seyfert 1.9 galaxy NGC 4565. This galaxy has a total radio flux density of 2.7 mJy at both 6 and 20 cm, as well as an upper limit to its diameter of  $d = 25$  pc. As an initial trial, we assume that the ionized gas is confined to a spherical volume of this size, centered on a point radio source. Therefore, the maximum path length  $L = d/2 = 12.5$  pc. Assuming uniform density along this line of sight, the density required to generate the estimated emission measure is  $n_e = 1000 - 1600 \text{ cm}^{-3}$ . However, for an ionized region 12.5 pc in radius with this density, the predicted H $\alpha$  luminosity for Case B recombination (Osterbrock 1989) would be at least  $8.5 \times 10^{40} \text{ erg s}^{-1}$ , far in excess of the observed value of  $2.8 \times 10^{38} \text{ erg s}^{-1}$  (Ho et al. 1997a). Therefore, the simplest picture is unlikely to be correct.

The above result is a manifestation of the well-known fact that the narrow-line regions of Seyferts must have filling factors for the ionized gas that are much smaller than unity (e.g., Osterbrock 1989, §11.5). In order to make the predicted and observed values of its H $\alpha$  luminosity consistent, it is necessary to decrease  $L$  and increase  $n_e$  relative to the initial assumption. Consider the case where we view the NGC 4565 radio source through the center of a single cloud of diameter  $L_{\text{pc}}$ , and assume an emission measure of  $E = 2 \times 10^7 \text{ cm}^{-3}$ , or a turnover frequency of 2.4 GHz. Then, both the spectral turnover and the observed H $\alpha$  luminosity could be accounted for by a path length of 1.6 pc and  $n_e = 3500 \text{ cm}^{-3}$ . Of course, it may be that the required amount of thermal gas would be broken up into

a number of smaller clouds which provide a similar total path length and volume. In any event, it appears that free-free absorption is a possible explanation for the flat spectrum only if the radio source is considerably smaller than the VLA upper limit of 25 pc.

As a check for self-consistency, we can predict the total free-free emission from the hypothetical absorbing cloud and compare it to the observed power from the NGC 4565 nucleus. The predicted free-free emission over all frequencies, from a 1.6-pc cloud with an ionized density of  $3500 \text{ cm}^{-3}$ , would be  $\sim 1.4 \times 10^{38} \text{ erg s}^{-1}$ . This luminosity would be contained in a free-free spectrum that should continue up to a frequency  $\nu \sim kT/h \sim 2 \times 10^{14} \text{ Hz}$  ( $1.5 \mu\text{m}$  wavelength). Assuming a thermal spectrum with spectral index  $-0.1$  from the estimated turnover frequency of 2.4 GHz up to  $2 \times 10^{14} \text{ Hz}$ , we predict a free-free flux density from the cloud of only  $\sim 20 \mu\text{Jy}$  at 2.4 GHz, less than 1% of the observed value of 2.7 mJy at gigahertz frequencies. Therefore, the radio data are consistent with the presence of the hypothetical obscuring cloud, but that cloud cannot account for the bulk of the radio emission. This is similar to the result found for radio-quiet quasars by Antonucci & Barvainis (1988).

The hypothesis of free-free absorption, which appears to be consistent with the observations to date, also might explain why the weak Seyfert 2 galaxies appear to be systematically weaker radio emitters in the Palomar sample than the Seyfert 1 galaxies, particularly at 20 cm. Free-free absorption from either the nuclear torus or the narrow-line region could be more important in the low-power Seyfert 2 galaxies. If absorption is associated with the torus, the apparent excess of flat- or inverted-spectrum objects in the weak Palomar Seyferts might occur if any radio jets present are too weak to punch their way out into the ionization cone, so that all the radio emission lies behind or within the torus. More powerful Seyferts, such as those in the distance-limited sample of Ulvestad & Wilson (1984b, 1989), would have radio emission extending outside the torus, and be less likely to be free-free absorbed. Using the models of Neufeld, Maloney, & Conger (1994), Wilson et al. (1998) showed that the spectral turnover of the Seyfert/LINER galaxy NGC 2639 could be accounted for by free-free absorption in the torus, either from a warm molecular gas phase or from a hot, weakly ionized atomic gas phase; the reader is referred to Wilson et al. (1998) for details. Alternatively, the absorption could be in the narrow-line region. Weak Seyferts might have more compact narrow-line regions, as appears to be the case for LINERs (Pogge et al. 2000). This could provide a larger covering factor of denser gas for the nuclear radio sources, again accounting for the putative increased absorption in the weaker objects.

Two possible radio tests exist for the free-free absorption hypothesis. First, very sensitive VLA imaging of the weakest radio sources in the Palomar Seyfert sample, at 3.6 cm or shorter wavelengths, could be used to attempt to detect the radio emission in the optically thin regime. In this regard, we note the apparent lack of obvious differences between radio properties of type 1 and type 2 Seyferts selected from infrared surveys (Thean et al. 2001; Schmitt et al. 2001a). Since the radio imaging of these samples was done at 3.6 cm, the published images might be relatively unaffected by free-free absorption, possibly being above the frequency of the absorption cutoff for most galaxies. Second, multi-frequency milliarcsecond-resolution VLBA imaging (not possible for the very weakest sources) could be used to search for multiple radio components

and measure their spectral shapes. We recently obtained such VLBA observations of three low-luminosity flat-spectrum active galaxies from the Palomar sample in order to carry out this search.

### 5. ARE THE DATA CONSISTENT WITH THE UNIFIED SCHEME?

We have carried out an analysis of a statistical sample of 45 Seyfert galaxies from the Palomar optical spectroscopic survey, for which high-resolution radio (VLA) observations were reported by Ho & Ulvestad (2001). The space density of such objects in galaxies having  $-22 \text{ mag} \leq M_{B_T} \leq -18 \text{ mag}$  is  $(1.25 \pm 0.38) \times 10^{-3} \text{ Mpc}^{-3}$ , about  $9\% \pm 3\%$  of the overall space density of bright galaxies. Previous surveys have identified Seyfert activity in a much smaller fraction of such galaxies. A variety of statistical tests have been carried out on the Palomar Seyfert sample in order to examine the consistency with the unified scheme for Seyfert galaxies. Here, we summarize some of the major points that have been brought out in the discussion and analysis.

First, the following points seem wholly consistent with the unified scheme:

1. The Seyfert 1 and Seyfert 2 galaxies appear in the same types of host galaxies.
2. There is no statistical difference in the forbidden-line luminosities or widths between Seyfert 1 and Seyfert 2 galaxies.
3. For the objects with stronger radio sources, the Seyfert 1 and Seyfert 2 galaxies obey the same radio-forbidden line relations.
4. The radio spectra of Seyfert 1 and Seyfert 2 galaxies are statistically consistent with each other.
5. Seyfert radio axes are uncorrelated with host galaxy axes.

There are a number of points that, taken at face value, seem inconsistent with the unified scheme. However, all have reasonable explanations in the classical scenario unifying Seyfert 1 and Seyfert 2 galaxies:

1. *Seyfert 1 galaxies appear to have more luminous radio sources than Seyfert 2 galaxies.* There are two possible explanations here. The first is a subtle selection bias, in which galaxies can only be identified as Seyfert 1 galaxies in the Palomar sample, or indeed in any sample selected by optical spectroscopy, if they have higher emission line equivalent widths, implying that the Seyfert 1 objects are identified systematically higher on the luminosity function. The second possible explanation is that the weak Seyfert 2 galaxies have a strong tendency to be absorbed.
2. *Weak Seyfert 2 galaxies have a smaller radio/[O III] ratio than weak Seyfert 1 galaxies.* This may be explained if a minimum level of nuclear activity is required to enable a radio jet to emerge from the vicinity of the central engine, and if the small radio sources below that minimum activity level are still contained inside or behind the nuclear torus.

3. *There is no correlation of radio source size with Seyfert type.* Only a relatively small fraction (20%–30%) of Seyfert galaxies have resolvable linear radio sources. The weaker active nuclei prevalent in the Palomar sample may not generate sources large enough to be resolved by the VLA, and our relatively small sample does not provide enough linear sources to expect any statistically significant difference.
4. *Seyfert 1 galaxies may contain a higher fraction of linear radio sources than Seyfert 2 galaxies.* This is consistent with a possible selection effect in which Seyfert 1 galaxies are identified higher on the luminosity function, if the more powerful objects are more likely to have linear sources.
5. *An apparently large fraction of Palomar Seyferts have flat spectra, when compared with previous samples of more powerful Seyferts.* This can be explained if the weaker objects contain no radio jets, or jets that are not powerful enough to blast out of the vicinity of the active nucleus. Then, the radio emission is hidden either behind the nuclear torus or behind a relatively compact narrow-line region, and can be free-free absorbed. An alternative possibility is that low-luminosity Seyferts undergo accretion with an ADAF, whose radio core has an inverted spectrum.

We conclude that all the properties of the Palomar Seyfert sample are consistent with the unified scheme for Seyferts *if* two conditions hold. First, there is some threshold level of Seyfert activity, below which the probability of a radio jet emerging from the nuclear region is small. Second, the lowest luminosity radio sources either are significantly free-free absorbed by ionized gas or are generated by highly sub-Eddington accretion flows.

We thank Neal Miller for assistance with the statistical tests, Mark Claussen for advice on plotting the figures, and Henrique Schmitt for useful discussions. We thank the referee, Ski Antonucci, for useful suggestions that helped clarify the paper. The National Radio Astronomy Observatory is a facility of the National Science Foundation, operated under cooperative agreement by Associated Universities, Inc. This research has made use of the NASA/IPAC Extragalactic Database (NED) which is operated by the Jet Propulsion Laboratory, California Institute of Technology, under contract with the National Aeronautics and Space Administration. In addition, this research has made use of NASA's Astrophysics Data System Abstract Service. The work of L. C. H. is partly funded by NASA grants HST-GO-06837.04-A, HST-AR-07527.03-A, and HST-AR-08361.02-A, awarded by the Space Telescope Science Institute, which is operated by AURA, Inc., under NASA contract NAS5-26555.

## REFERENCES

Antonucci, R. R. J. 1993, *ARA&A*, 31, 473

Antonucci, R., & Barvainis, R. 1988, *ApJ*, 332, L13

Antonucci, R. R. J., & Miller, J. S. 1985, *ApJ*, 297, 621

Barvainis, R., Lonsdale, C., & Antonucci, R. 1996, *AJ*, 111, 1431

Bicknell, G. V., Dopita, M. A., Tsvetanov, Z. I., & Sutherland, R. S. 1998, *ApJ*, 495, 680

Bower, G. A., Wilson, A., Morse, J. A., Gelderman, R., Whittle, M., & Mulchaey, J. 1995, *ApJ*, 454, 106

Busko, I. C., & Steiner, J. E. 1992, *MNRAS*, 258, 306

Capetti, A., Axon, D. J., & Macchetto, F. D. 1997, *ApJ*, 487, 560

Clark, D. H., & Caswell, J. L. 1976, *MNRAS*, 174, 267

Condon, J. J. 1989, *ApJ*, 338, 13

—. 1992, *ARA&A*, 30, 575

Condon, J. J., Anderson, M. L., & Helou, G. 1991, *ApJ*, 376, 95

de Bruyn, A. G., & Wilson, A. S. 1976, *A&A*, 53, 93

—. 1978, *A&A*, 64, 433

de Grijp, M. H. K., Keel, W. C., Miley, G. K., Goudfrooij, P., & Lub, J. 1992, *A&AS*, 96, 38

Edelson, R. 1987, *ApJ*, 313, 651

Evans, I. N., Koratkar, A. P., Allen, M., Dopita, M., & Tsvetanov, Z. 1999, *ApJ*, 521, 531

Falcke, H., Lehár, J., Barvainis, R., Nagar, N. M., & Wilson, A. S. 2001, in *Probing the Physics of Active Galactic Nuclei by Multiwavelength Monitoring*, ASP Conf. Ser., ed. B. M. Peterson, R. S. Polidan, & R. W. Pogge (San Francisco: ASP), in press (astro-ph/0009457)

Falcke, H., Nagar, N. M., Wilson, A. S., & Ulvestad, J. S. 2000, *ApJ*, 542, 197

Falcke, H., Wilson, A. S., & Simpson, C. 1998, *ApJ*, 502, 199

Feigelson, E. D., & Nelson, P. I. 1985, *ApJ*, 293, 192

Ferland, G. J., & Osterbrock, D. E. 1986, *ApJ*, 300, 658

Giuricin, G., Mardirossian, F., Mezzetti, M., & Bertotti, G. 1990, *ApJS*, 72, 551

Heckman, T. M., Miley, G. K., van Breugel, W. J. M., & Butcher, H. R. 1981, *ApJ*, 247, 403

Helou, G., Soifer, B. T., & Rowan-Robinson, M. 1985, *ApJ*, 298, L7

Hewett, P. C., Foltz, C. B., & Chaffee, F. H. 1995, *ApJ*, 406, L43

Ho, L. C., Filippenko, A. V., & Sargent, W. L. W. 1993a, *ApJ*, 417, 63

—. 1995, *ApJS*, 98, 477

—. 1997a, *ApJS*, 112, 315

—. 1997b, *ApJ*, 487, 568

Ho, L. C., Filippenko, A. V., Sargent, W. L. W., & Peng, C. Y. 1997c, *ApJS*, 112, 391

Ho, L. C., & Peng, C. Y. 2001, *ApJ*, in press (astro-ph/01020502)

Ho, L. C., Rudnick, G., Rix, H.-W., Shields, J. C., McIntosh, D. H., Filippenko, A. V., Sargent, W. L. W., & Eracleous, M. 2000, *ApJ*, 541, 120

Ho, L. C., Shields, J. C., & Filippenko, A. V. 1993b, *ApJ*, 410, 567

Ho, L. C., & Ulvestad, J. S. 2001, *ApJS*, 133, 77

Huchra, J. P., & Burg, R. 1992, *ApJ*, 393, 90

Huchra, J., & Sargent, W. L. W. 1973, *ApJ*, 186, 433

Hyman, S. D., Lacey, C. K., Weiler, K. W., & Van Dyk, S. D. 2000, *AJ*, 119, 1711

Isobe, T., & Feigelson, E. D. 1990, *BAAS*, 22, 917

Kinney, A. L., Schmitt, H. R., Clarke, C. J., Pringle, J. E., Ulvestad, J. S., & Antonucci, R. R. J. 2000, *ApJ*, 537, 152

Kukula, M. J., Pedlar, A., Baum, S. A., & O'Dea, C. P. 1995, *MNRAS*, 276, 1262

Lacey, C., Duric, N., & Goss, W. M. 1997, *ApJS*, 109, 417

Lasota, J.-P., Abramowicz, M. A., Chen, X., Krolik, J., Narayan, R., & Yi, I. 1996, *ApJ*, 462, 142

LaValley, M., Isobe, T., & Feigelson, E. D. 1992, in *Astronomical Data Analysis Software and Systems I*, ASP Conf. Ser. 25, ed. D. M. Worrall, C. Biemesderfer, & J. Barnes (San Francisco: ASP), 245

Levinson, A., Laor, A., & Vermeulen, R. C. 1995, *ApJ*, 448, 589

Mahadevan, R. 1997, *ApJ*, 477, 585

Markarian, B. E., Lipovetskij, V. A., & Stepanian, J. A. 1981, *Astrophysics*, 17, 321

Meurs, E. J. A., & Wilson, A. S. 1984, *A&A*, 136, 206

Mezger, P. G., & Henderson, A. P. 1967, *ApJ*, 147, 471

Moran, E. C., Barth, A. J., Kay, L. E., & Filippenko, A. V. 2000, *ApJ*, 540, L73

Morganti, R., Tsvetanov, Z. I., Gallimore, J., & Allen, M. G. 1999, *A&AS*, 137, 457

Nagar, N. M., & Wilson, A. S. 1999, *ApJ*, 516, 97

Nagar, N. M., Wilson, A. S., Mulchaey, J. S., & Gallimore, J. F. 1999, *ApJS*, 120, 209

Narayan, R., Mahadevan, R., & Quataert, E. 1998, in *The Theory of Black Hole Accretion Discs*, ed. M. A. Abramowicz, G. Björnsson, & J. E. Pringle (Cambridge: Cambridge Univ. Press), 148

Narayan, R., Yi, I., & Mahadevan, R. 1995, *Nature*, 374, 623

Neff, S. G., & Ulvestad, J. S. 2000, *AJ*, 120, 670

Neufeld, D. A., Maloney, P. R., & Conger, S. 1994, *ApJ*, 436, L127

Osterbrock, D. E. 1989, *Astrophysics of Gaseous Nebulae and Active Galactic Nuclei* (Mill Valley: Univ. Science Books)

Pedlar, A., Booher, R. V., Spencer, R. E., & Stewart, O. J. 1983, *MNRAS*, 202, 647

Perley, R. A. 2000, *BAAS*, 32, 1574

Peterson, B. M. 1993, *PASP*, 105, 247

Peterson, B. M., & Wandel, A. 2000, *ApJ*, 540, L13

Pogge, R. W., Maoz, D., Ho, L. C., & Eracleous, M. 2000, *ApJ*, 532, 323

Quataert, E., Di Matteo, T., Narayan, R., & Ho, L. C. 1999, *ApJ*, 525, L89

Roy, A. L., Colbert, E. J. M., Wilson, A. S., & Ulvestad, J. S. 1998, *ApJ*, 504, 147

Roy, A. L., Norris, R. P., Kesteven, M. J., Troup, E. R., & Reynolds, J. E. 1994, *ApJ*, 432, 496

Sandage, A. R., & Tammann, G. A. 1981, *A Revised Shapley-Ames Catalog of Bright Galaxies* (Washington, DC: Carnegie Inst. of Washington) (RSA)

Sandage, A. R., Tammann, G. A., & Yahil, A. 1979, *ApJ*, 232, 352

Sanders, D. B., Phinney, E. S., Neugebauer, G., Soifer, B. T., & Matthews, K. 1989, *ApJ*, 347, 29

Schmidt, M. 1968, *ApJ*, 151, 393

Schmitt, H. R., Antonucci, R. R. J., Ulvestad, J. S., Kinney, A. L., Clarke, C. J., & Pringle, J. E. 2001a, *ApJ*, in press (astro-ph/0103263)

Schmitt, H. R., Kinney, A. L., Storchi-Bergmann, T., & Antonucci, R. 1997, *ApJ*, 477, 623

Schmitt, H. R., Ulvestad, J. S., Antonucci, R. R. J., & Kinney, A. L. 2001b, *ApJS*, 132, 199

Thean, A., Pedlar, A., Kukula, M. J., Baum, S. A., & O'Dea, C. P. 2000, *MNRAS*, 314, 573

—. 2001, *MNRAS*, in press (astro-ph/0103266)

Thompson, A. R., Clark, B. G., Wade, C. M., & Napier, P. J. 1980, *ApJS*, 44, 151

Tran, H. D. 1995, *ApJ*, 440, 597

Ulvestad, J. S., & Antonucci, R. R. J. 1997, *ApJ*, 488, 621

Ulvestad, J. S., & Wilson, A. S. 1984a, *ApJ*, 278, 544

—. 1984b, *ApJ*, 285, 439

—. 1989, *ApJ*, 343, 659

Ulvestad, J. S., Wrobel, J. M., Roy, A. L., Wilson, A. S., Falcke, H., & Krichbaum, T. P. 1999, *ApJ*, 517, L81

Unger, S. W., Lawrence, A., Wilson, A. S., Elvis, M., & Wright, A. E. 1987, *MNRAS*, 228, 521

Veilleux, S., & Osterbrock, D. E. 1987, *ApJS*, 63, 295

Walker, R. C., Dhawan, V., Romney, J. D., Kellermann, K. I., & Vermeulen, R. C. 2000, *ApJ*, 530, 233

Wandel, A., Peterson, B. M., & Malkan, M. A. 1999, *ApJ*, 526, 579

Whittle, M. 1985, *MNRAS*, 213, 33

—. 1992a, *ApJ*, 387, 109

—. 1992b, *ApJ*, 387, 121

Whittle, M., Haniff, C. A., Ward, M. J., Meurs, E. J. A., Pedlar, A., Unger, S. W., Axon, D. J., & Harrison, B. A. 1986, *MNRAS*, 222, 189

Williams, P. J. S. 1963, *Nature*, 200, 56

Wills, B. J. 1999, in *Quasars and Cosmology*, ASP Conf. Ser. 162, ed. G. Ferland & J. Baldwin (San Francisco: ASP), 101

Wilson, A. S. 1991, in *The Interpretation of Modern Synthesis Observations of Spiral Galaxies*, ASP Conf. Ser. 18, ed. N. Duric & P. C. Crane (San Francisco: ASP), 227

Wilson, A. S., & Tsvetanov, Z. I. 1994, *AJ*, 107, 1227

Wilson, A. S., & Willis, A. G. 1980, *ApJ*, 240, 429

Wilson, A. S., et al. 1998, *ApJ*, 505, 587

Wrobel, J. M., & Herrnstein, J. R. 2000, *ApJ*, 533, L111

TABLE 1  
OPTICAL LUMINOSITY FUNCTION  
FOR PALOMAR SEYFERTS

$M_{B_r}^a$ (mag)	$\log \phi$ ( $\text{Mpc}^{-3}\text{mag}^{-1}$ )	No.
-18.25	$-3.17^{+0.23}_{-0.56}$	2
-18.75	...	0
-19.25	$-3.18^{+0.14}_{-0.22}$	7
-19.75	$-3.59^{+0.16}_{-0.27}$	5
-20.25	$-3.57^{+0.13}_{-0.17}$	11
-20.75	$-3.92^{+0.13}_{-0.20}$	9
-21.25	$-4.43^{+0.19}_{-0.36}$	4
-21.75	$-5.08^{+0.20}_{-0.39}$	3

<sup>a</sup>Total (nucleus + host galaxy) magnitude. Bins outside the tabulated range include no more than one galaxy each, and are not shown.

TABLE 2  
RADIO LUMINOSITY FUNCTIONS FOR PALOMAR SEYFERTS

$\log P^a$ ( $\text{W Hz}^{-1}$ )	6 cm		20 cm	
	$\log \phi$ ( $\text{Mpc}^{-3}\text{mag}^{-1}$ )	No.	$\log \phi$ ( $\text{Mpc}^{-3}\text{mag}^{-1}$ )	No.
19.0	$-4.32^{+0.20}_{-0.39}$	3.3	...	...
19.4	$-3.38^{+0.21}_{-0.42}$	7.7	$-3.57^{+0.28}_{-1.07}$	2
19.8	$-4.09^{+0.22}_{-0.48}$	4	$-4.54^{+0.21}_{-0.42}$	3
20.2	$-3.94^{+0.19}_{-0.36}$	4	$-3.87^{+0.19}_{-0.37}$	4
20.6	$-4.81^{+0.23}_{-0.53}$	2	$-4.26^{+0.21}_{-0.41}$	4
21.0	$-4.21^{+0.19}_{-0.37}$	6	$-4.22^{+0.20}_{-0.38}$	5
21.4	$-4.31^{+0.20}_{-0.42}$	6	$-5.38^{+0.20}_{-0.38}$	3
21.8	$-4.62^{+0.23}_{-0.53}$	2	$-4.34^{+0.22}_{-0.45}$	4
22.2	...	0	$-4.49^{+0.20}_{-0.38}$	3

<sup>a</sup>Bins outside the tabulated range include no more than one galaxy each, and are not shown.

TABLE 3  
SUMMARY OF STATISTICAL TESTS

Independent Variable	Dependent Variable	Statistical Significance <sup>a</sup>	Section
Seyfert type	Distance	54%	3.1
Seyfert type	Core 20 cm power	0.9%	3.4.1
Seyfert type	Total 20 cm power	0.9%	3.4.1
Seyfert type	Core 6 cm power	2.0%	3.4.1
Seyfert type	Total 6 cm power	1.3%	3.4.1
Seyfert type	[O III] luminosity	15%	3.5
Seyfert type	Total 20 cm/[O III] ratio	0.9%	3.5
Seyfert type	20 cm/[O III], strong [O III]	51%	4.2
Seyfert type	20 cm/[O III], weak [O III]	1.3%	4.2
Seyfert type	20 cm/[O III], weak [O III], no E gal.	0.1%	4.2
Seyfert type	Total 6 cm/[O III] ratio	1.2%	3.5
Seyfert type	6 cm/[O III], strong [O III]	26%	4.2
Seyfert type	6 cm/[O III], weak [O III]	3.1%	4.2
Seyfert type	6 cm/[O III], weak [O III], no E gal.	0.6%	4.2
Seyfert type	Total spectral index	29%	3.6
Seyfert type	Peak spectral index	63%	3.6
Seyfert type	Radio size, resolved	74%	3.7
Seyfert type	Radio size, all	31%	3.7
Seyfert type	Radio morphology	9.2%	3.8
Seyfert type	Radio morphology, incl. Ambiguous	2.9%	3.8
Seyfert type	$q = \text{FIR}/\text{radio}$ ratio	1.3%	4.2
Seyfert type	H $\alpha$ equivalent width	0.8%	4.3
Host-galaxy type	Seyfert type	48%	3.2
[O III] luminosity	Total 20 cm power	< 0.01%	3.5
[O III] luminosity	Total 6 cm power	< 0.01%	3.5
[N II] line width	Total 20 cm power	< 0.01%	3.5
[N II] line width	Total 6 cm power	< 0.01%	3.5
Total 6 cm power	Radio morphology	8.8%	3.8
Total 6 cm power	Radio morphology, incl. Ambiguous	1.4%	3.8

<sup>a</sup>The statistical significance of differences between the two Seyfert types is generally defined as the probability that the distributions of the dependent variable would differ by the observed amount if the two Seyfert types were drawn from the same parent population.

TABLE 4  
SEYFERT SAMPLES IMAGED IN THE RADIO AT ARCSECOND RESOLUTION

Name	Selection	No.	Observations	Resolution	References
Markarian	UV excess	29	VLA: 6, 20 cm	0."/4–1."/3	1
Distance-limited	Heterogeneous	57	VLA: 6, 20 cm	0."/4–1."/3	2
CFA	Optical	47	VLA: 3.6 cm	0."/2–2."/0	3
Southern	Heterogeneous	29	VLA, ATCA: 3.5, 6 cm	1."/0	4
12- $\mu$ m	Infrared	107	VLA: 3.6 cm	0."/25	5
60- $\mu$ m	Infrared	75	VLA: 3.6 cm	0."/25	6
Palomar	Optical	45	VLA: 6, 20 cm	1."/1	7

References. — (1) Ulvestad & Wilson 1984a; (2) Ulvestad & Wilson 1984b, 1989; (3) Kukula et al. 1995; (4) Morganti et al. 1999; (5) Thean et al. 2000, 2001; (6) Kinney et al. 2000, Schmitt et al. 2001a, 2001b; (7) Ho & Ulvestad 2001, this paper.